Biophysical Characterization of Triacyl Monosaccharide Lipid A Partial Structures in Relation to Bioactivity

Klaus Brandenburg,* Motohiro Matsuura,† Holger Heine,* Mareike Müller,* Makato Kiso,‡ Hideharu Ishida,‡ Michel H. J. Koch,§ and Ulrich Seydel*

*Forschungszentrum Borstel, Division of Biophysics, D-23845 Borstel, Germany; †Department of Microbiology, Jichi Medical School, Tochigi 329-0498, Japan; ‡Department of Applied Bioorganic Chemistry, Gifu University, Gifu 501-1193, Japan; and §European Molecular Biology Laboratory EMBL c/o DESY, D-22603 Hamburg, Germany

ABSTRACT Synthetic triacyl glucosamine monosaccharide lipid A part structures corresponding to the non-reducing moiety of enterobacterial lipid A with an acyloxyacyl chain linked to position 3 of the glucosamine and an unbranched chain linked to position 2 (group 1) and vice versa (group 2) were analyzed biophysically: Fourier-transform infrared spectroscopy was performed to characterize the gel-to-liquid crystalline phase transition, the phosphate band contour, and the orientation of the glucosamine with respect to the membrane surface. Small-angle x-ray diffraction was applied for the elucidation of the supramolecular aggregate structure and, with that, of the molecular shape. With fluorescence resonance energy transfer the lipopolysaccharide-binding protein (LBP)-mediated intercalation of the lipid A partial structures into phospholipid liposomes was monitored. The physical data clearly exhibit a classification of the synthetic compounds into two groups: group 1 compounds have sharp phase transitions, indicating dense acyl chain packing and an inclination of the glucosamine backbone with respect to the membrane surface of 30° with the phosphate buried in the membrane. Group 2 compounds have a very broad phase transition, indicating poorly packed acyl chains, and an inclination of −30° with the phosphate group sticking outward. For the first group unilamellar phases are observed superimposed by a non-lamellar structure, and for the second one only multilamellar aggregate structures. The cytokine-inducing capacity in human mononuclear cells is relatively high for the first group and low or absent for the second group. Based on these data a model of the intra and intermolecular conformations is proposed which also extends the concept of "endotoxic conformation."

INTRODUCTION

Lipopolysaccharides (LPS), the endotoxins of Gram-negative bacteria, consist of an oligo or polysaccharide chain covalently linked to a lipid moiety termed lipid A. Lipid A has been shown to constitute the "endotoxic principle" of LPS (Zähringer et al., 1994), although in some biological test systems its activity was found to be significantly lower than that of the parent LPS (Schromm et al., 1998). It was furthermore found that lipid A variants exist that deviate from the common structure of enterobacterial lipid A, a diphosphoryl diglucosamine acylated with up to seven hydroxylated fatty acid residues in ester or amide linkage. These lipid A variants are found, for example, in *Rhodobacter capsulatus* having only five acyl chains (and a length, on the average, of only C-12) and exhibiting no biological activity despite an identical diglucosamine backbone (Krauss et al., 1989). These observations raised questions about the structural requirements for the induction of endotoxicity. It was found that the minimal structure of lipid A expressing biological activity is a backbone composed of two hexosamine saccharides, which are substituted by two phosphates and six asymmetrically distributed fatty acids with appropriate chain lengths, preferentially C-14 as present in lipid A from *Escherichia coli* (Rietschel et al., 1996). The dependence of biological activity on the chemical structure of lipid A-like samples was studied in detail using various synthetic lipid A analogs and partial structures (Imoto et al., 1984, 1987; Kiso et al., 1987a). These compounds exhibited patterns of different biological activities in human cells ranging from high endotoxicity for compound "506," a counterpart of the natural hexaacyl lipid A from *Escherichia coli*, to complete inactivity for compound "406," corresponding to the tetraacyl lipid A precursor Ia or IVa (Galanos et al., 1985; Homma et al., 1985; Kotani et al., 1985; Loppnow et al., 1986).

Previously it was reported that some monosaccharide-type lipid A partial structures exhibited LPS-mimetic activities such as cytokine-inducing activity in murine macrophages and induction of resistance to microbial infections and tumors in animal models (Nakatsuka et al., 1989; Ikeda et al., 1990). Furthermore, it was shown that certain triacyl monosaccharide-type lipid A partial structures (GLA-60 and GLA-63) were able to act agonistically not only in murine, but also in human macrophages, although they were two orders less active than hexaacyl *E. coli*-type lipid A "506" (Funatogawa et al., 1998; Matsuura et al., 1999). In the present study a series of structurally related triacyl monoglucosamine lipid A partial structures corresponding to the non-reducing part of the lipid A diglucosamine backbone, carrying a phosphate group in position 4, were investigated with the aim of characterizing the relationship between their physicochemical behavior and biological (endotoxic) activity. One group consists of the glucosamine

Submitted October 22, 2001, and accepted for publication March 14, 2002.

Address reprint requests to Dr. K. Brandenburg, Forschungszentrum Borstel, D-23845 Borstel, Germany. Tel.: +49-4537-188235; Fax: +49-4537-188632; E-mail: kbranden@fz-borstel.de.

0006-3495/02/07/322/12 $2.00

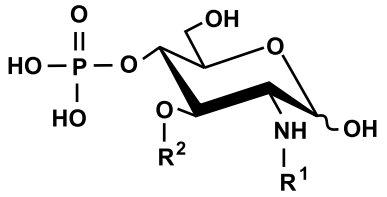

		R^1	R^2
Group 2	GLA 27	14:0 [3-O(14:0)]	14:0
	GLA 58	14:0 [3-O(16:0)]	14:0
	GLA 59	14:0 [3-O(14:0)]	14:0 (3-OH)
Group 1	GLA 60	14:0 (3-OH)	14:0 [3-O(14:0)]
	GLA 68	14:0	14:0 [3-O(14:0)]
	GLA 69	14:0	14:0 [3-O(16:0)]

FIGURE 1 Chemical structures of the monosaccharide triacyl lipid A partial structures. The compounds with the acyloxyacyl residue linked to R^2 are called group 1, those with the acyloxyacyl residue linked to R^1 are called group 2 glycolipids.

partial structure with an acyloxyacyl chain linked to position 2 and an unbranched acyl chain to position 3, and the other group with the reversed linkage. Fourier-transform infrared spectroscopy (FTIR) was applied for the characterization of the $\beta \leftrightarrow \alpha$ gel-to-liquid crystalline phase behavior of the hydrocarbon chains deduced from the position of the symmetric stretching vibrational band of the methylene groups, and for the intramolecular and intermolecular conformations from vibrational bands in the backbone such as phosphate and glucosamine ring modes, also using dichroic measurements with polarized IR light. Synchrotron radiation small-angle x-ray diffraction was applied for the determination of the aggregate structure, from which the molecular shape can be derived. This information is of importance since it was found that a conical shape of the lipid A molecules is directly related to biological activity (Brandenburg et al., 1993, 1996; Schromm et al., 1998, 2000). Biological activity was monitored by the ability of the compounds to 1) activate tumor necrosis factor α (TNF-α) in human mononuclear cells, 2) activate the *Limulus polyphemus* clotting cascade, and 3) to bind to CD14 or to the Toll-like receptors TLR2 and TLR4 in a CHO reporter cell line.

From these investigations a model of the molecular conformations of the glycolipid partial structures and information about molecular prerequisites for endotoxic activity can be derived.

MATERIALS AND METHODS

Lipids and reagents

Monosaccharide lipid A part structures in the triethylamine salt form were synthesized chemically as described elsewhere (Kiso et al., 1987a,b). Their chemical structure is given in Fig. 1. Note that the structures of the compounds represent pairwise mirror images of their acyl chain residues, GLA-27 and GLA-68, GLA-58 and GLA-69, and GLA-60 and GLA-59, respectively. The compounds with the acyloxyacyl residue in position 3 (R^2) are called group 1 glycolipids, and those substituted in position 2 (R^1) are called group 2 glycolipids.

The analogs were shown not to contain any detectable contaminants such as disaccharide analogs by reverse-phase high-performance liquid chromatography analysis. Free lipid A from *E. coli* was isolated by acetate buffer treatment of deep rough mutant LPS from strain WBB01 (kindly provided by W. Brabetz, Research Center Borstel). After isolation, the resulting lipid A was purified and converted to its triethylamine salt. MALDI-TOF mass spectrometry proved that this preparation contained only hexaacyl lipid A without any tetra or pentaacyl subfractions. 3-*sn*-Phosphatidylserine, egg 3-*sn*-phosphatidylcholine, sphingomyelin from bovine brain, and 3-*sn*-phosphatidylethanolamine from *E. coli* were from Avanti Polar Lipids, Inc. (Birmingham, AL). The synthetic lipopeptide Pam_3CSK_4 (palmitoyl$_3$-cystein-serine-lysine$_4$) was kindly provided by EMC microcollectors (Tübingen, Germany).

Sample preparation

The lipid samples were usually prepared as aqueous dispersions with a high, i.e., above 85%, buffer content using 20 mM HEPES. For this, the lipids were suspended directly in buffer and temperature-cycled several times between 5 and 70°C and then stored for at least 12 h before measurement. For preparation of liposomes from the phospholipid mixture resembling the composition of the cell membrane of macrophages ($PL_{M\phi}$)—3-*sn*-phosphatidylcholine, 3-*sn*-phosphatidylserine, 3-*sn*-phosphatidylethanolamine, and sphingomyelin in a molar ratio of 1:0.4:0.7:0.5 (Kröner et al., 1981)—the lipids were solubilized in chloroform, the solvent was evaporated under a nitrogen stream, and afterward completely removed in vacuo and the lipids were resuspended in the appropriate volume of buffer and further treated as described for LPS.

FTIR

The infrared spectra were recorded on a 5-DX FTIR spectrometer (Nicolet Instruments, Madison, WI) and on an IFS-55 (Bruker, Karlsruhe, Germany) spectrometer essentially as described earlier (Brandenburg et al., 1997). Briefly, in transmission measurements the samples were placed in a CaF_2 cuvette with a 12.5-μm-thick Teflon spacer. Temperature scans were performed automatically in the range of 10–70°C with a heating rate of 0.6°C/min. In the case of weak absorption bands, resolution enhancement techniques like Fourier self-deconvolution (Kauppinen et al., 1981) were applied after baseline subtraction. In the case of overlapping bands, in particular for the analysis of the phosphate band contour, curve-fitting was applied using a modified version of the CURFIT procedure (D. Moffat, NRC, Ottawa, Canada). Beside the transmission experiments, for the determination of the infrared dichroism with polarized light the lipid samples were also prepared as oriented thin multilayers, as described previously (Seydel et al., 2000). The lipid sample was placed into a closed cuvette and the air above the sample was saturated with water vapor to maintain full hydration. Infrared ATR spectra were recorded with a mercury-cadmium-telluride (MCT) detector with a scan number of 1000 and a resolution of 2 cm^{-1}.

To determine the angle θ between the diglucosamine diphosphorylated backbone and the membrane surface, the dichroic ratio R must be measured and the order parameter S must be estimated. R is obtained from the ratio of the peak areas of the absorption bands of the vertically and horizontally polarized IR light. The order parameter of the acyl chains ($S = 1$ for perfectly aligned and $S = 0$ for isotropically distributed molecules) can be estimated from the peak position of the symmetric stretching vibration $\nu_s(CH_2)$ (Seydel et al., 2000). Because the hydrocarbon chains of the lipid multilayer are homogenously distributed around the normal to the ATR plate ("partial axial distribution"), a tilt of the backbone with respect to the

direction of the acyl chains leads to a broader distribution of the backbone, and the estimation of S provides an upper limit.

X-ray diffraction

X-ray diffraction measurements were performed at the European Molecular Biology Laboratory (EMBL) outstation at the Hamburg synchrotron radiation facility HASYLAB using the double-focusing monochromator-mirror camera X33 (Koch and Bordas, 1983) as described earlier (Brandenburg et al., 1998). Briefly, diffraction patterns in the range of the scattering vector $0.07 < s < 1$ nm^{-1} ($s = 2 \sin \theta/\lambda$, 2θ scattering angle, and λ the wavelength, 0.15 nm) were recorded with exposure times of 2 or 3 min using a linear detector with delay line readout (Gabriel, 1977).

The relevant aggregate structures are lamellar and cubic structures, which can be characterized by the following features. 1) Lamellar: the reflections are grouped in equidistant ratios, i.e., at 1, 1/2, 1/3, 1/4, etc., of the lamellar repeat distance d_l. 2) Cubic: these are nonlamellar three-dimensional structures. Their various space groups differ in the ratio of their spacings. The relation between reciprocal spacing $s_{hkl} = 1/d_{hkl}$ and lattice constant a is

$$s_{hkl} = (h^2 + k^2 + l^2)^{1/2}/a$$

where hkl are Miller indices of the corresponding set of plane.

Fluorescence resonance energy transfer (FRET) spectroscopy

The FRET assay was performed as described earlier (Schromm et al., 1996; Gutsmann et al., 2000). Briefly, phospholipid liposomes corresponding to the composition of the macrophage membrane ($PL_{M\phi}$) were doubly labeled with the fluorescent dyes *N*-(7-nitrobenz-2-oxa-1,3-diazol-4yl)-phosphatidylethanolamine (NBD-PE) and *N*-(lissamine rhodamine B sulfonyl)-phosphatidylethanolamine (Rh-PE) (Molecular Probes, Eugene, OR). Intercalation of unlabeled molecules into the doubly labeled liposomes leads to probe dilution, and with that to a lower FRET efficiency: the emission intensity of the donor increases and that of the acceptor decreases (for clarity, only the donor emission intensity is shown here).

In all experiments doubly labeled PS liposomes were prepared, and after 50 s the lipids and after 100 s LBP were added, each at a final concentration of 0.01 mM, and the NBD donor fluorescence intensity at 531 nm was monitored for at least 300 s.

Chromogenic *Limulus* test of endotoxin activity

Endotoxin activity of the lipids in the concentration range 10 μg/ml down to 1 ng/ml was determined by a quantitative kinetic assay based on the reactivity of Gram-negative endotoxin with *Limulus* amebocyte lysate (LAL) (Friberger et al., 1987), using test kits from BioWhittaker (Walkersville, MD 50-650U).

In this assay, the amount of 14 endotoxin units (EU)/ml corresponds to 1 ng/ml wild-type LPS O55:B5, at 50 EU/ml the system is in saturation, and the sensitivity limit is <0.2 EU/ml.

Stimulation of human mononuclear cells (MNC)

Human mononuclear cells were stimulated with the lipids, and the TNF-α production of the cells was determined in the supernatant to establish the cytokine-inducing capacity of the lipids.

For the isolation of MNC, heparinized (20 IE/ml) blood was taken from healthy donors and processed directly by mixing it with an equal volume of Hanks' balanced solution and centrifugation on a Ficoll density gradient for 40 min (21°C, 500 × g). The interphase layer of mononuclear cells was collected and washed twice in Hanks' medium, and once in serum-free RPMI 1640 containing 2 mM L-glutamine, 100 U/ml penicillin, and 100 g/ml streptomycin. The cells were resuspended in serum-free medium and their number was equilibrated at $5 \cdot 10^6$ cells/ml. For stimulation, 200 μl/well MNC ($5 \cdot 10^6$ cells/ml) were transferred into 96-well culture plates. The stimuli were serially diluted in pyrogen-free sterile water and added to the cultures at 20 μl/well. The cultures were incubated for 4 h at 37°C under 6% CO_2. Supernatants were collected after centrifugation of the culture plates for 10 min at 400 × g and stored at −20°C until determination of cytokine content.

TNF in the cell supernatant was determined immunologically in a sandwich-ELISA; 96-well plates (Greiner, Solingen, Germany) were coated with a monoclonal antibody against TNF (clone 6b from Intex AG, Switzerland). Cell culture supernatants and the standard (recombinant TNF, Intex) were diluted with buffer. After exposure to appropriately diluted test samples and serial dilutions of standard rTNF, the plates were exposed to peroxidase-conjugated rabbit anti-rTNF antibody. The plates were shaken 16–24 h at 4°C. For the removal of free antibodies, the plates were washed six times in distilled water. Subsequently, the color reaction was started by addition of tetramethylbenzidine/H_2O_2 in alcoholic solution and stopped after 5–15 min by the addition of 1 N sulfuric acid. In the color reaction the substrate is cleaved enzymatically, and the product can be measured photometrically. This was done on an ELISA reader (Rainbow, Tecan, Crailsham, Germany) at a wavelength of 450 nm, and the values were related to the standard.

Activation of CHO reporter cells

The CHO/CD14 reporter line, clone 3E10, is a stably transfected CD14-positive CHO (Chinese hamster ovary) cell line that expresses inducible membrane CD25 (Tac antigen) under transcriptional control of the human E-selectin promoter (pELAM.Tac (Delude et al., 1998)). The promoter fragment chosen contains an essential nuclear factor (NF)-κB binding site (Schindler and Baichwal, 1994). The CHO/CD14/huTLR2 reporter cell line was constructed by stable cotransfection of 3E10 with the cDNA for human TLR2 and pcDNA3 (Invitrogen, Yoshimura et al., 1999). The CHO reporter cell line EL1 was obtained by stable cotransfection of CHO-K1 cells with the plasmid pCEP4 (Invitrogen) and pELAM.Tac. CHO cell lines were grown in Ham's F12 medium containing 10% FCS and 1% penicillin/streptomycin at 37°C in a humidified 5% CO_2 environment. Medium was supplemented with 400 U of hygromycin B/ml and 0.5 mg of G418/ml (CHO/CD14/huTLR2).

Flow cytometry analysis of NF-κB activity

Cells were plated at a density of 2.5×10^5/well in 24-well dishes. The following day the cells were stimulated as indicated in Ham's F12 medium containing 10% FCS (total volume of 0.3 ml/well). Subsequently, the cells were harvested with trypsin-EDTA, labeled with FITC-CD25 mAb (Dako, Germany) and analyzed by flow cytometry.

RESULTS

$\beta \leftrightarrow \alpha$ acyl chain melting

The temperature dependence of the peak position of the symmetric stretching vibration $\nu_s(CH_2)$ is shown in Fig. 2. From these data the gel-to-liquid crystalline ($\beta \leftrightarrow \alpha$) phase transition of the acyl chains can be determined that is lipid-specific and indicative of acyl chain order (Mantsch and McElhaney, 1991). From Fig. 2, a strong dependence of the phase transition temperature T_c on the chemical struc-

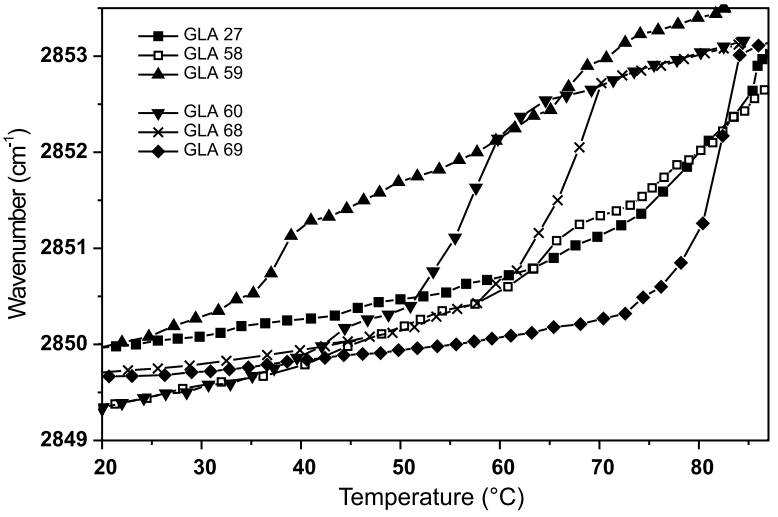

FIGURE 2 Temperature dependence of the peak position of the symmetric stretching vibration of the methylene groups $\nu_s(CH_2)$ for all six GLA compounds, monitoring the gel-to-liquid crystalline ($\beta \leftrightarrow \alpha$) phase behavior of the hydrocarbon chains.

ture can be deduced. Importantly, the glycolipids from group 2 (GLA-27, GLA-58) exhibit a very broad phase transition ($T_c \sim 77°C$) or even two transitions (GLA-59, $T_{c1} = 38°C$, $T_{c2} = 68°C$). In contrast, the compounds from group 1 have sharp phase transitions (GLA-60, $T_c = 56°C$; GLA-68, $T_c = 67°C$; GLA-69, $T_c = 82°C$).

Phosphate vibration

The peak position of antisymmetric stretching vibration of the negatively charged phosphate $\nu_{as}(PO_2^-)$ gives information about the degree of hydration of the phosphate group. The spectral range 1300–1160 cm^{-1} comprising the $\nu_{as}(PO_2^-)$ and the wagging progression bands $\gamma_w(CH_2)$ is plotted in Fig. 3 for the lipids GLA-27 and GLA-68 at some selected temperatures. At lower temperatures, the gel-phase specific $\gamma_w(CH_2)$-bands are prominent, in particular for GLA-27, but they vanish above T_c. To study the phosphate band components, which have components at 1200–1260 cm^{-1} depending on the state of hydration (Fringeli and Günthard, 1981), the spectra at the highest temperatures were evaluated by subtracting a baseline between 1300 and 1160 cm^{-1} and fitting the curves of the individual components. The results shown for GLA-27 and GLA-68 in Fig. 4 clearly indicate different hydration states: phosphate band components corresponding to weak or no hydration at 1250–1270 cm^{-1} are significantly expressed for GLA-68 but absent for GLA-27, whereas the components typical for highly hydrated phosphate groups are strong for GLA-27 but only moderate for GLA-68. For a quantitative estimate, the peak area of the invariant glucosamine ring vibrational band at 1185–1190 cm^{-1} was set to 100%. For GLA-27, the peak area of the two components at 1200 and 1220 cm^{-1} correspond to 47% of the glucosamine band intensity and 35% for GLA-68, and the band at the higher wavenumber, which is absent for GLA-27, corresponds to 46%. Summarizing the data for all GLA compounds, they can be classified into two groups: The phosphate band contours of group 1 have a considerable contribution from a dehydrated state, whereas the group 2 glycolipids have not.

Infrared-ATR spectroscopy with polarized light

The lipids were investigated as hydrated multilayers in an attenuated total reflectance (ATR) unit utilizing polarized light for a more detailed analysis of various functional

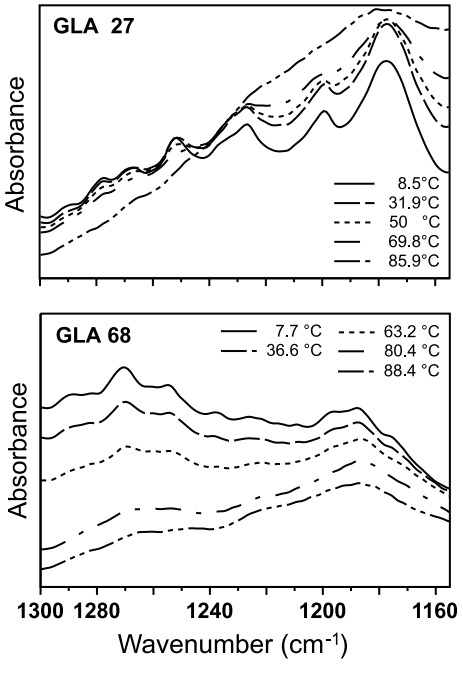

FIGURE 3 Infrared spectra in the wavenumber range 1300–1160 cm^{-1} for GLA-27 (*top*) and GLA-68 (*bottom*) at different temperatures. In this range, the antisymmetric stretching vibration of the negatively charged phosphate $\nu_{as}(PO_2^-)$ is found, which is superimposed to the wagging progression bands $\gamma_w(CH_2)$ typical for the gel phase of lipids.

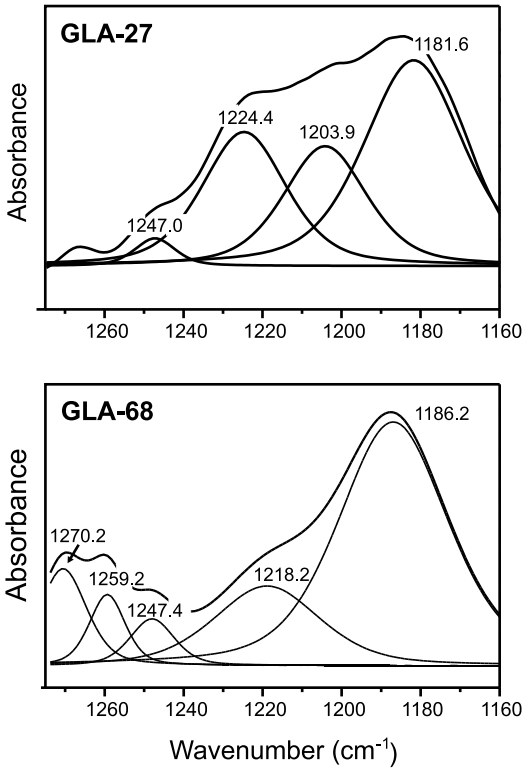

FIGURE 4 Infrared spectra for GLA-27 at 85.9°C (*top*) and GLA-68 at 88.4°C (*bottom*) in the wavenumber range 1300–1160 cm^{-1} after baseline subtraction and individual band components after curve-fitting (using the CURFIT procedure from the NRC, Ottawa, with a Gauss/Lorentz ratio of 0.6). The glucosamine ring mode is taken as intensity standard of 100%.

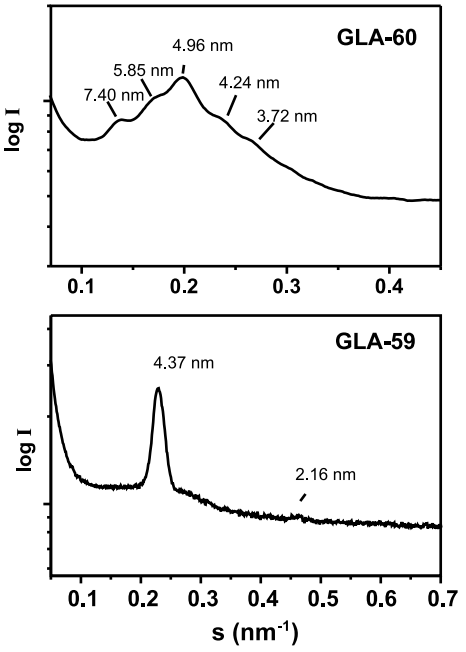

FIGURE 5 Synchrotron radiation x-ray diffraction patterns of GLA-60 (*top*) and GLA-59 (*bottom*) at 90% water content and 40°C. The logarithm of the scattering intensity log I is plotted versus the scattering vector $s = 2 \sin \theta/\lambda$ (2θ = scattering angle, λ = wavelength = 0.15 nm).

groups, in particular with respect to their orientation behavior. The dichroic ratios of vibrational bands from the glucosamine backbone at 1170, 1085, and 1045 cm^{-1} were evaluated to determine the inclination angle θ between the backbone and the membrane surface (Seydel et al., 2000). The results for the different glycolipids are listed in Table 1. The error $\Delta\theta$ is obtained from the error ΔR (=0.02) and ΔS, for which a high value of 0.12 was assumed.

From these results it can be concluded that the glucosamine backbone of all glycolipids have an inclination angle of ~30° with respect to the membrane surface; however, the angle is positive for group 1 (the phosphate is located in the membrane plane), and negative for group 2 glycolipids (the phosphate is outside the membrane plane).

TABLE 1 Inclination angle Θ of the glucosamine backbone with respect to the membrane surface from the measured dichroic ratios *R* of the glucosamine ring vibrations (ΔR = 0.02) and assuming $S = 0.85 \pm 0.12$

Compound	Inclination Angle Θ
GLA-27	+29.0 ± 4.2
GLA-58	+30.5 ± 2.4
GLA-59	+31.2 ± 2.5
GLA-60	−28.5 ± 6.5
GLA-68	−31.6 ± 4.7
GLA-69	−34.1 ± 1.9

Small-angle x-ray scattering (SAXS)

The lipids were investigated by synchrotron radiation SAXS to determine their three-dimensional supramolecular aggregate structure. The diffraction patterns, i.e., the logarithm of the scattering intensity log I versus scattering vector *s*, at 90% water content and 40°C are shown in Fig. 5 for GLA-60 (*top*) and GLA-59 (*bottom*). For the latter and the two other glycolipids of group 2 with the acyloxyacyl chain linked to the 2-position, the patterns consist of sharp reflections in equidistant ratios typical for multilamellar structures. The periodicity characteristic for the length of the acyl chains is highest for GLA-58 (d_1 = 4.70 nm), slightly lower for GLA-27 (4.62 nm), and lowest for GLA-59 (4.37 nm, Fig. 5). Interestingly, the presence of the 3-OH group in the acyl chain linked to the 3-position (GLA-59) leads to a significantly shorter bilayer periodicity as compared to the sample without OH group (GLA-27).

In contrast, the group 1 glycolipids with the acyloxyacyl chain in the 3-position have more complex patterns, which are indicative of a main lamellar phase superimposed by a non-lamellar structure. Thus, the diffraction pattern of GLA-60 (Fig. 5) shows a broad band between $S = 0.12$ nm^{-1} and 0.30 nm^{-1} centered around 0.2 nm^{-1}. Considering the fact that the band contour shows nearly no changes

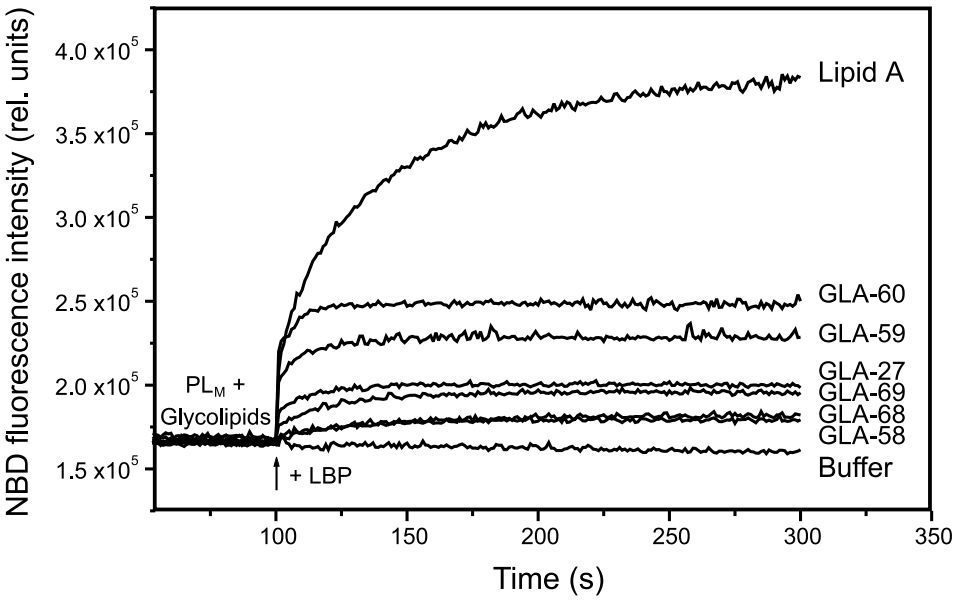

FIGURE 6 Fluorescence resonance energy transfer (FRET) spectroscopic measurement of doubly labeled liposomes $PL_{M\phi}$ corresponding to the composition of the macrophage membrane with the GLA-lipids added after 50 s and lipopolysaccharide-binding protein (LBP) after 100 s. The donor (NBD-PE) fluorescence intensity at 531 nm is shown versus time. The final concentrations of the glycolipids and LBP are 10^{-5} molar, the temperature is 37°C.

up to temperatures of 70°C (not shown), there is evidence for the existence of unilamellar vesicles or multilamellar structures with large interbilayer spacings (Lewis and Engelman, 1983). The basic pattern, however, is superimposed by reflections that may be assigned to a cubic phase. If a value of 14.5 ± 0.4 nm is taken as the (nonobservable) periodicity a_Q, then the reflections may be grouped according to 7.40 nm = $a_Q/\sqrt{4}$, 5.85 nm = $a_Q/\sqrt{6}$, 4.96 nm = $a_Q/\sqrt{9}$, 4.24 nm = $a_Q/\sqrt{12}$, and 3.72 nm = $a_Q/\sqrt{16}$. Compound GLA-60 thus probably adopts a cubic substructure of space group Q^{224} commonly found for lipid A-like compounds (Brandenburg et al., 1990, 1998). The two other glycolipids of group 1 (GLA-68, GLA-69) exhibit similar complex diffraction patterns resulting from a lamellar phase superimposed by reflections not compatible with a lamellar phase (data not shown). These are, however, not readily assignable, as in the case of GLA-60.

FRET spectroscopy

Fluorescence resonance energy transfer (FRET) spectroscopy was applied at 37°C for the detection of a lipopolysaccharide-binding protein (LBP)-mediated intercalation of the glycolipids into target membranes, such as a phospholipid membrane corresponding to the composition of the macrophage membrane $PL_{M\phi}$. From Fig. 6 it can be deduced that after addition of LBP at $t = 100$ s to the coincubated $PL_{M\phi}$ and GLA compounds, a lipid-specific increase of the NBD-fluorescence intensity is observed corresponding to an intercalation into $PL_{M\phi}$, which is highest for lipid A. Interestingly, for the GLA-lipids the strength of intercalation depends on the presence of 3-OH groups: isomers GLA-58 and GLA-69 with the longest acyl chains and isomers GLA-27 and GLA-68 without OH group intercalate less than the isomers GLA-59 and GLA-60 with 3-OH-groups.

Cytokine induction in human mononuclear cells

The ability of the lipids to induce TNF-α production in human mononuclear cells was tested for various concentrations and compared with lipid A from *E. coli*. Two points are worth mentioning: first, lipid A is by two orders of magnitude more active than the compounds GLA-60 and GLA-68 (data not shown). Second, again a classification in two groups is possible: the group 1 glycolipids display activity in the 1–100 μg/ml concentration range, while the group 2 glycolipids are inactive, except for a small activity of GLA-27. These results are illustrated by listing the amount of glycolipid necessary to induce 200 pg/ml of TNF-α (Fig. 7).

Limulus amebocyte lysate

The ability of the lipids to activate the *Limulus* amebocyte lysate clotting cascade was not different for the glycolipids of the two groups, as shown exemplarily for GLA-27, GLA-58, and GLA-69 in Fig. 8. Down to concentrations of 1 ng/ml, lipid A has a slightly higher activity (data not shown).

CHO reporter system

To investigate the potential involvement of the membrane proteins of immune cells, CD14, TLR2, and TLR4, in the recognition of the glycolipids, we analyzed the stimulatory activity of the GLA compounds in a CHO cell reporter

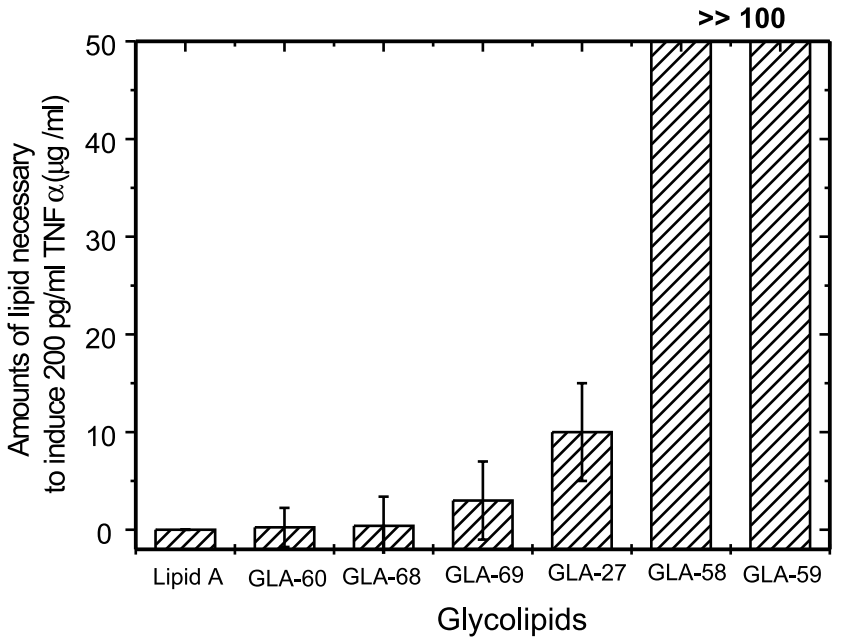

FIGURE 7 Amount of lipid A or GLA compounds (in μg/ml) necessary to induce the release of 200 pg/ml TNF-α from human mononuclear cells. The error bars (standard deviation) result from the determination of TNF-α in duplicate at two different dilutions. The data are representative of four independent measurements.

system (Fig. 9). Upon induction of NF-κB translocation in these reporter cells, human CD25 is expressed on the cell surface. The data clearly indicate that neither expression of TLR4 (EL1) alone or coexpression of CD14 and TLR4 (3E10), nor expression of CD14, TLR2, and TLR4 (3E10hTLR2) is sufficient to enable the cells to respond to the GLA compounds. As controls, stimulation of the different cell lines with either LPS (S-form from *Salmonella friedenau*) or lipopeptide LP (Pam_3CSK_4) showed the expected phenotype, TLR4 reactivity for LPS, and TLR2 reactivity for the lipopeptide.

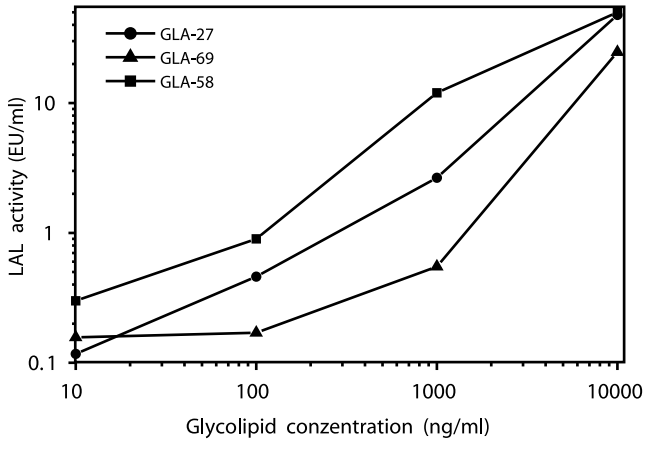

FIGURE 8 Endotoxin activity in the chromogenic *Limulus* amebocyte lysate assay in the concentration range 10 ng/ml to 10 μg/ml for GLA-27, GLA-58, and GLA-69. A value of 14 endotoxin units (EU)/ml corresponds to 1 ng/ml LPS (S-form from *Salmonella friedenau*). At 50 EU/ml the system is in saturation, and the sensitivity limit is <0.2.

DISCUSSION

The data above clearly illustrate that the monophosphoryl triacyl monosaccharide partial structures of lipid A corresponding to its non-reducing moiety can be grouped into two classes: for the group 1 glycolipids the sharp gel-to-liquid crystalline phase transitions (Fig. 2) indicate an acyl chain packing typical for saturated lipids, whereas the broad phase transitions observed for the group 2 lipids, typical for biological membrane lipids differing in length and saturation of the acyl chains, indicate a much lower acyl chain order that could be due to coexisting phases, to a less dense packing of the hydrocarbon chains, and/or to a much lower cooperativity of the chain melting. For a variety of LPS and lipid A and lipid A part structures, the broadness of the phase transition has never been observed to exceed 10–15°C (Brandenburg et al., 1990, 1997). A lack of cooperativity connected with poor acyl chain packing might be due to the unfavorable arrangement of neighboring molecules that might be disoriented relative to each other, because the backbones are not parallel aligned. This can be deduced directly from the evaluation of the conformations of the phosphate groups: analysis of the phosphate band contour $\nu_{as}(PO_2^-)$ indicates strong hydration of the phosphate group of the group 2 glycolipids, while for the group 1 glycolipids the occurrence of band components due to undisturbed vibrations are indicative of a dehydrated phosphate group (Figs. 3 and 4). Furthermore, the group 2 glycolipids adopt multilamellar structures, in contrast to the group 1 glycolipids, with diffraction spectra corresponding to superpositions of a mainly lamellar (unilamellar or multilamellar with large interbilayer spacings) with a non-lamellar structure,

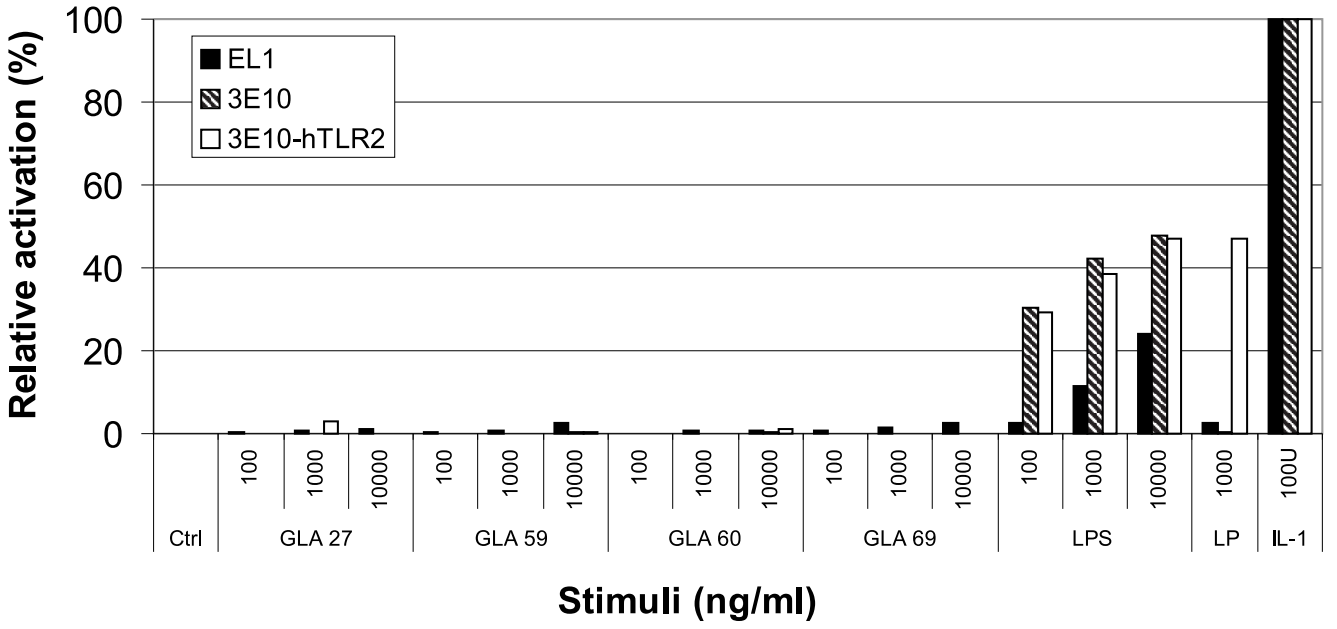

FIGURE 9 Relative activation rate of CHO reporter cells stimulated by GLA compounds, LPS S-form from *Salmonella friedenau*, synthetic lipopeptide (LP = Pam_3CSK_4), and interleukin 1 (IL-1). In each cell line the CD25 expression induced by 100 U/ml of IL-1 signal was set to 100%.

which can be assigned to cubic phase Q^{224} for GLA-60 (Fig. 5). As an explanation for the occurrence of a lamellar with a cubic substructure for the group 1 glycolipids coexisting phases may be assumed, although these are difficult to imagine for homogenous compounds. Cubic structures have been assumed to exist exclusively in disordered (liquid crystalline) phases of the acyl chains (Luzzati, 1997). The occurrence of these structures in the gel phase is an unusual finding; however, that seems to be typical for LPS- and lipid A-like structures, as reported previously (Brandenburg et al., 1990, 1998) and was explained by the higher fluidities (lower state of order) of these compounds in the gel phase as compared to, e.g., saturated phospholipids. These findings were supported by the considerably lower enthalpy change ΔH_c at the phase transition, indicating a partial fluidization already below the phase transition temperature (T_c) and by wide-angle x-ray diffraction studies, indicating a much higher value of the main wide-angle reflection for endotoxins (0.43–0.45 nm) as compared to saturated phospholipids (0.405–0.42 nm). Because the former investigations also gave evidence for the occurrence of mixed lamellar/non-lamellar phases (Brandenburg et al., 1998), the question of the occurrence of a cubic phase in the gel state of the hydrocarbon chains may only be of hypothetical character: in the FTIR experiment of the phase behavior (Fig. 2), the more fluid cubic substructure within a main lamellar structure in the gel phase may not be visible.

In the literature, transitions from lamellar into non-lamellar structures have been reported to take place in the liquid crystalline phase. For example, the $L \rightarrow H_{II}$ transition of natural phosphatidylethanolamine expresses in the symmetric stretching mode by a change in the wavenumber values from 2852.5 to 2853.5 cm^{-1} (Casal and Mantsch, 1984). No infrared data, however, seem to be available for the different cubic structures of lipids.

From the aggregate structures of the lipids, it is possible to deduce the molecular shape of the individual molecules (Schromm et al., 2000). Thus, the existence of a multilamellar structure is typical for amphiphiles with a cylindrical shape having identical cross-sections of the hydrophilic and hydrophobic moieties. From non-lamellar structures a conical shape of the molecules can be derived with a larger cross-section of the hydrophobic moiety than of the hydrophilic one. Together with the finding that for all GLA compounds an inclination angle of ~30° (Table 1) of the glucosamine backbone with respect to the membrane surface is found, a model for the intra and intermolecular conformation of the GLA-structures can be deduced (Fig. 10). In this model, the inclination of +30° of the GlcN backbone with the phosphate group buried in the membrane leads to a slightly conical shape of the molecule and a dense acyl chain packing of the glycolipids of group 1, whereas the inclination of the GlcN backbone with the phosphate sticking into the environment of −30° leads to a cylindrical shape and a much looser acyl chain packing in the case of the glycolipids of group 2. Interestingly, this model implies that the more ordered chains of the group 1 glycolipids seem to occupy a greater cross-sectional area. This apparent paradoxon might be understood in light of the fact that the phosphate groups of the group 1 glycolipids are buried in the membrane interior, probably via hydrogen binding with

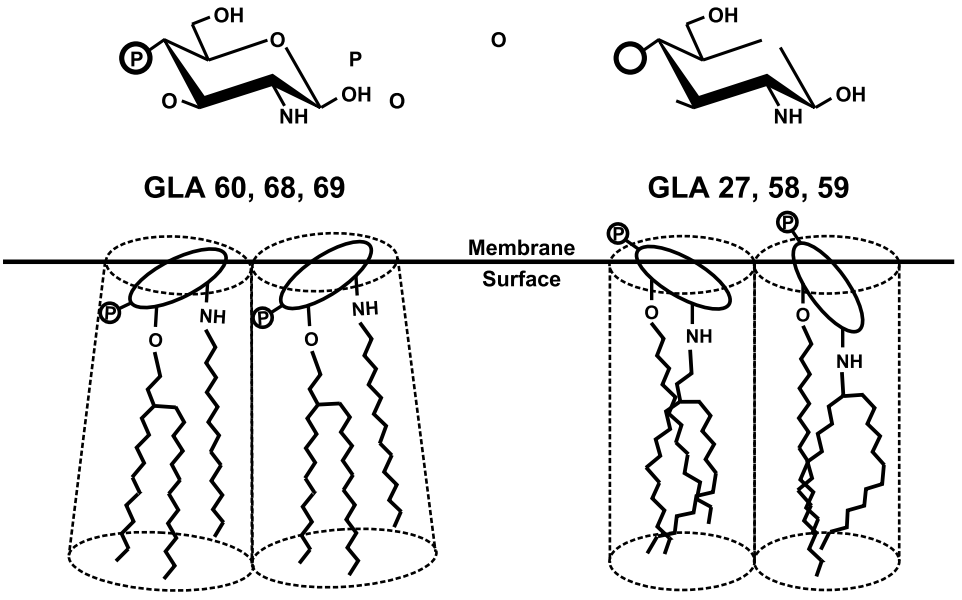

FIGURE 10 Model of the intra and intermolecular conformations of the GLA compounds. For the group 1 glycolipids the binding is stabilized by hydrogen bonding between the phosphate group and neighboring molecules. In contrast, for the group 2 glycolipids the absence of an interaction of the phosphate group with neighboring molecules leads to high conformational disorder. The outward-oriented phosphates, however, lead to the formation of multibilayers in contrast to the behavior of the group 1 glycolipids.

neighboring molecules, thus reducing the effective cross-section of the headgroup.

The different orientation of the phosphate groups may also serve as explanation for the different swelling behavior of the two groups: for the group 2 glycolipids the outward-oriented phosphates are able to bridge adjacent bilayers via cation binding, thus allowing the lipid aggregates to pack into multilamellar structures. The cation bridging may be due to the action of the triethylamine salt, but may also be supported by cations from the buffer solution.

In contrast, for the group 1 glycolipids the membrane-incorporated phosphates do not allow the formation of a multilamellar structure. This way, the question of the assignment of the broad diffraction bands of the group 1 glycolipids to a unilamellar or a multilamellar structure with large interbilayer spacing can now be answered in favor of the former.

It should be emphasized that for the entire hexacyl lipid A molecule with four acyl chains at the non-reducing and two at the reducing glucosamine, an inclination of the diglucosamine of ~50° with the 4′-phosphate buried in the membrane and the 1-phosphate sticking into the environment was observed (Brandenburg et al., 1997; Seydel et al., 2000). Thus, the conformation of the group 1 glycolipids corresponds to the conformation of the non-reducing moiety of whole lipid A.

The comparison of the lamellar periodicities of the group 2 glycolipids GLA-27, GLA-58, and GLA-59 (Fig. 5) with those of lipid A (which adopts lamellar phases only at higher Mg^{2+} concentrations; Brandenburg et al., 1990) is interesting. The spacings of the first reflection for the GLA compounds are between 4.37 and 4.70 nm, being much lower than for lipid A (around 5.50 nm), although the medium chain lengths of the GLA compounds are even longer than that of lipid A. One possibility could be the different swelling of these glycolipids, i.e., different fluid spacings between adjacent bilayers. However, it was found that lipid A under nearly dehydrated conditions (water content 0–10%) has a periodicity of 4.9–5.0 nm (Brandenburg et al., 1990), being still significantly above the values for the GLA compounds. Thus, we assume that the strong inclination angle of the diglucosamine backbone with respect to the membrane surface of >50° for lipid A (Seydel et al., 2000), i.e., nearly a factor of two larger than for the monosaccharide compounds, is responsible for this significant difference. Another possibility, however, cannot be ruled out: a hydrocarbon chain tilt can be the cause of the lower periodicities of the group 2 glycolipids, which would lead to a decrease of the observed spacings similar to those found for phosphatidylcholine (McIntosh, 1980).

It should be noted that the IR-ATR experiments had to be performed at much lower water content as hydrated multibilayers than the x-ray diffraction measurements. Since for lipid A a profound lyotropic behavior was found (Brandenburg et al., 1990)—lamellar at lower and non-lamellar structures at higher water content—the corresponding data cannot necessarily be correlated. It was reported, however, that the inclination of the backbone for various lipid A and part structures is exclusively influenced by "intramolecular packing," i.e., packing constraints of the isolated molecules with the tendency of the acyl chains to pack parallel and thus to force the backbone to incline. This inclination is not influenced by neighboring molecules (Seydel et al., 2000) and is thus independent of the water content.

Concomitantly with the marked differences of the physicochemical parameters, the two groups of GLA compounds differ in the biological response, with a relatively high cytokine-inducing capacity of group 1 and no or only mar-

ginal activity of group 2 (Fig. 7). It should be noted, however, that significant biological activity toward mononuclear cells is found only at concentrations that are two orders of magnitude higher than for lipid A. This difference may result, at least partially, from differences in the tendency to adopt non-lamellar structures, and thus a conical molecular shape: this is strong for lipid A, weak for the group 1, and absent for the group 2 glycolipids.

In contrast to the findings in the cytokine assay, the *Limulus polyphemus* test system does not differentiate between the different glycolipids (Fig. 8), i.e., both groups yield identical reactions. This finding is in accordance with the results for lipid A- and LPS-protein mixtures, for which a concentration-dependent decrease or increase of LAL activity was found independent of the results in the cellular test (Jürgens et al., 2001; Brandenburg et al., 2001). Also, the characterization of the interaction of endotoxins with cationic liposomes indicated no change in the LAL assay despite a strong electrostatic attraction (Poxon and Hughes, 1999). In a previous paper, various synthetic lipid A analogs and partial structures were tested in the *Limulus* test using three different assays. A dependence in particular on the presence of 3-OH groups was found, and the results obtained in the colorimetric test also correlated better with a pyrogenicity test in rabbits than that observed by the gelation method, although the dependence on the chemical structure was most expressed by the pyrogenicity test (Takada et al., 1988). Asai et al. (1998) examined the LAL activity of the endotoxin antagonist E5531, a synthetic lipid A structure based on that of natural *Rhodobacter capsulatus* lipid A and found high activity, although it did not induce cytokines and even acted antagonistically in the pyrogenicity test. Therefore, the *Limulus* test is not suitable for a quantitative determination of endotoxin-induced bioactivity, such as cytokine-inducing capacity. Furthermore, there is still a lot of uncertainty as to the endotoxin target structures in the LAL test.

An important question is the mechanism of interaction of endotoxins with the target cell membrane of immune cells leading to cell signaling. It was found that the acute-phase serum protein LBP binds to the endotoxins and transfers them directly into the membrane (Schromm et al., 1996) or to the membrane-anchored LPS-receptor mCD14 (Tobias and Ulevitch, 1993; Mathison et al., 1992). Because mCD14 is anchored only by a phosphatidylinositol, this receptor cannot transfer a signal across the membrane. Other proteins, such as the TLR (Yang et al., 1998; Chow et al., 1999; Lien et al., 2000), CD55 (El-Samalouti et al., 1999), ion channels (Blunck et al., 2001), or heat-shock proteins (Triantafilou et al., 2001) must contribute to signal transduction. In the case of TRL2 and TRL4, at least one more protein, MD2, must be present for signaling (Shimazu et al., 1999; Dziarski et al., 2001; Schromm et al., 2001), and recent experiments indicate the contribution of an entire protein cluster (Triantafilou et al., 2001).

We proposed earlier that a prerequisite for cell activation (Blunck et al., 2001) is the intercalation of the endotoxin molecules into the membrane of target cells. This can be mediated directly by LBP, as illustrated in Fig. 6, or by the action of other soluble or membrane-proteins, such as sCD14 or mCD14. Intercalation alone is, however, not sufficient for cell activation. As can be seen from Fig. 6, the active and inactive compounds are intercalated into the liposomal membrane by LBP, and the amount of intercalated molecules is determined by the individual acyl chain substituents rather than the position, 2 or 3, to which they are linked. However, the compounds carrying a 3-OH fatty acid chain (GLA-59, GLA-60) intercalate most effectively (Fig. 6). Not surprisingly, all of the GLA compounds intercalate less effectively than lipid A, in accordance with previous findings that the amount of intercalation decreases with decreasing number of negative charges (Schromm et al., 1998).

When intercalated into the membrane, only those endotoxins with a conical molecular shape cause a sufficiently strong disturbance at the site of the signaling cascade protein, thus initiating cell signaling. A very promising candidate for this is the ion channel MaxK, which is known to be stress-sensitive (Seydel et al., 2001; Blunck et al., 2001). Similarly to the finding for complete lipid A, only the GLA compounds with at least a slight tendency for a conical conformation are able to induce this stress.

This is not necessarily the only possible mechanism of cell activation. An alternative approach of the observed differences between the two glycolipid classes could be the difference in the aggregate structure. The group 1 glycolipids mainly form unilamellar structures, and the potential binding groups within the glycolipids may be readily accessible for the serum and membrane proteins mentioned above. In contrast, for the group 2 glycolipids, with their multilamellar structure, most of the possible binding structures are hidden and thus are not available for binding to the proteins.

The experiments with different CHO reporter cells with the GLA compounds gave some rather surprising results. Because CHO cells are natural TLR2 null mutants (Heine et al., 1999), this system easily allows the identification of TLR2-dependent ligands. As can be seen after stimulation with a synthetic lipopeptide, only the TLR2-transfected 3E10hTLR2 cells respond (Fig. 9). However, none of the GLA compounds is able to induce translocation of NF-κB in these cells, allowing the conclusion that neither CD14 or TLR2 nor TLR4 are sufficient to induce activation by GLA compounds, and thus strongly implicates other or additional signaling molecules in the activation pathway of GLA glycolipids.

We are indebted to G. von Busse and U. Diemer for performing IR spectroscopic and LAL activity measurements, respectively.

This work was financially supported by the Deutsche Forschungsgemeinschaft (SFB 367/B8 and Br 1070/2-1).

REFERENCES

Asai, Y., K. Iwamoto, and S. Watanabe. 1998. The effect of the lipid A analog E5531 on phospholipid membrane properties. *FEBS Lett.* 438: 15–20.

Blunck, R., O. Scheel, M. Müller, K. Brandenburg, U. Seitzer, and U. Seydel. 2001. New insights into endotoxin-induced activation of macrophages: involvement of a K^+ channel in transmembrane signaling. *J. Immunol.* 166:1009–1015.

Brandenburg, K., G. Jürgens, M. Müller, S. Fukuoka, and M. H. J. Koch. 2001. Biophysical characterization of lipopolysaccharide and lipid A inactivation by lactoferrin. *Biol. Chem.* 382:1215–1225.

Brandenburg, K., M. H. J. Koch, and U. Seydel. 1990. Phase diagram of lipid A from *Salmonella minnesota* and *Escherichia coli* rough mutant lipopolysaccharide. *J. Struct. Biol.* 105:11–21.

Brandenburg, K., S. Kusumoto, and U. Seydel. 1997. Conformational studies of synthetic lipid A analogues and partial structures by infrared spectroscopy. *Biochim. Biophys. Acta.* 1329:193–201.

Brandenburg, K., H. Mayer, M. H. J. Koch, J. Weckesser, E. T. Rietschel, and U. Seydel. 1993. Influence of the supramolecular structure of free lipid A on its biological activity. *Eur. J. Biochem.* 218:555–563.

Brandenburg, K., W. Richter, M. H. J. Koch, H. W. Meyer, and U. Seydel. 1998. Characterization of the nonlamellar cubic and H_{II} structures of lipid A from *Salmonella enterica* serovar Minnesota by x-ray diffraction and freeze-fracture electron microscopy. *Chem. Phys. Lipids.* 91:53–69.

Brandenburg, K., U. Seydel, A. B. Schromm, H. Loppnow, M. H. J. Koch, and E. T. Rietschel. 1996. Conformation of lipid A, the endotoxic center of bacterial lipopolysaccharide. *J. Endotox. Res.* 3:173–178.

Casal, H. L., and H. H. Mantsch. 1984. Polymorphic phase behaviour of phospholipid membranes studied by infrared spectroscopy. *Biophys. Biochim. Acta.* 779:381–401.

Chow, J. C., D. W. Young, D. T. Golenbock, W. J. Christ, and F. Gusovsky. 1999. Toll-like receptor-4 mediates lipopolysaccharide-induced signal transduction. *J. Biol. Chem.* 274:10689–10692.

Delude, R. L., A. Yoshimura, R. R. Ingalls, and D. T. Golenbock. 1998. Construction of a lipopolysaccharide reporter cell line and its use in identifying mutants defective in endotoxin, but not TNF-α, signal transduction. *J. Immunol.* 161:3001–3009.

Dziarski, R., Q. L. Wang, K. Miyake, C. J. Kirschning, and D. Gupta. 2001. MD-2 enables Toll-like receptor 2 (TLR2)-mediated responses to lipopolysaccharide and enhances TLR2-mediated responses to Gram-positive and Gram-negative bacteria and their cell wall components. *J. Immunol.* 166:1938–1944.

El-Samalouti, V. T., J. Schletter, I. Chyla, A. Lentschat, U. Mamat, L. Brade, H.-D. Flad, A. J. Ulmer, and L. Hamann. 1999. Identification of the 80 kDa LPS-binding protein (LMP80) as decay accelerating factor (DAF, CD55). *FEMS Immunol. Med. Microbiol.* 23:259–269.

Friberger, P., L. Sörskog, K. Nilsson, and M. Knös. 1987. The use of a quantitative assay in endotoxin testing. *In* Detection of Bacterial Endotoxin with the Limulus Amebocyte Lysate Test. S. W. Watson, J. Levin, and T. J. Novitzky, editors. A. Liss, New York. 149–169.

Fringeli, U. P., and H. H. Günthard. 1981. Infrared membrane spectroscopy. *In* Membrane Spectroscopy. E. Grell, editor. Springer-Verlag, Berlin. 270–332.

Funatogawa, K., M. Matsuura, M. Nakano, M. Kiso, and A. Hasegawa. 1998. Relationship of structure and biological activity of monosaccharide lipid A analogs to induction of nitric oxide production by murine macrophage RAW264.7 cells. *Infect. Immun.* 66:5792–5798.

Gabriel, A. 1977. Position-sensitive x-ray detector. *Rev. Sci. Instrum.* 48:1303–1305.

Galanos, C., O. Lüderitz, E. T. Rietschel, O. Westphal, H. Brade, L. Brade, M. Freudenberg, U. Schade, M. Imoto, H. Yoshimura, S. Kusumoto, and T. Shiba. 1985. Synthetic and natural *Escherichia coli* free lipid A express identical endotoxic activities. *Eur. J. Biochem.* 148:1–5.

Gutsmann, T., A. B. Schromm, M. H. J. Koch, S. Kusumoto, K. Fukase, M. Oikawa, U. Seydel, and K. Brandenburg. 2000. Lipopolysaccharide-binding protein-mediated interaction of lipid A from different origin with phospholipid membranes. *Phys. Chem. Chem. Phys.* 2:4521–4528.

Heine, H., C. J. Kirschning, E. Lien, B. G. Monks, M. Rothe, and D. T. Golenbock. 1999. Cutting edge: cells that carry a null allele for Toll-like receptor 2 are capable of responding to endotoxin. *J. Immunol.* 162: 6591–6595.

Homma, J. Y., M. Matsuura, S. Kanegasaki, Y. Kawakubo, Y. Kojima, N. Shibukawa, Y. Kumazawa, A. Yamamoto, K. Tanamoto, T. Yasuda, M. Imoto, H. Yoshimura, S. Kusumoto, and T. Shiba. 1985. Structural requirement of lipid A responsible for the function: a study with chemically synthesized lipid A and its analogs. *J. Biochem.* 98:395–406.

Ikeda, S., M. Matsuura, M. Nakatsuka, J. Y. Homma, M. Kiso, A. Hasegawa, and C. Nishimura. 1990. Non-specific protective activity of synthetic lipid A-subunit analogs against microbial infections is influenced by their 2-*N*- and 3-*O*-linked acyl substituents in the D-glucosamine backbone. *J. Clin. Lab. Immunol.* 32:177–181.

Imoto, M., N. Yoshimura, S. Kusumoto, and T. Shiba. 1984. Total synthesis of lipid A, active principle of bacterial endotoxin. *Proc. Jpn. Acad. Ser. B.* 60:285–288.

Imoto, M., H. Yoshimura, T. Shimamoto, N. Sakaguchi, S. Kusumoto, and T. Shiba. 1987. Total synthesis of *Escherichia coli* lipid A, the endotoxically active principle of cell-surface lipopolysaccharide. *Bull. Chem. Soc. Jpn.* 60:2205–2214.

Jürgens, G., M. Müller, M. H. J. Koch, and K. Brandenburg. 2001. Interaction of hemoglobin with enterobacterial lipopolysaccharide and lipid A: physicochemical characterization and biological activity. *Eur. J. Biochem.* 268:4233–4242.

Kauppinen, J. K., D. J. Moffat, H. H. Mantsch, and D. G. Cameron. 1981. Fourier self-deconvolution: a method for resolving intrinsically overlapped bands. *Appl. Spectrosc.* 35:271–276.

Kiso, M., S. Tanaka, M. Fujishima, Y. Ogawa, and A. Hasegawa. 1987b. Synthesis of nonreducing sugar subunit analogues of bacterial lipid A carrying an amide-bound (3R)-3-acyloxytetradecanoyl group. *Carbohydr. Res.* 162:247–256.

Kiso, M., S. Tanaka, M. Fujita, Y. Fujishima, Y. Ogawa, H. Ishida, and A. Hasegawa. 1987a. Synthesis of the optically active 4-*O*-phosphono-D-glucosamine derivatives related to the non-reducing sugar subunit of bacterial lipid A. *Carbohydr. Res.* 162:127–140.

Koch, M. H. J., and J. Bordas. 1983. X-ray diffraction and scattering on disordered systems using synchrotron radiation. *Nucl. Instr. Meth.* 208: 461–469.

Kotani, S., H. Takada, M. Tsujimoto, T. Ogawa, I. Takahashi, T. Ikeda, K. Otsuka, H. Shimaguchi, N. Kasai, J. Mashimo, S. Nagao, A. Tanaka, S. Tanaka, K. Harada, K. Nagaki, H. Kitamura, T. Shiba, S. Kusumoto, M. Imoto, and H. Yoshimura. 1985. Synthetic lipid A with endotoxic and related biological activities comparable to those of a natural lipid A from *Escherichia coli* Re-mutant. *Infect. Immun.* 49:225–237.

Krauss, J. H., U. Seydel, J. Weckesser, and H. Mayer. 1989. Structural analysis of the nontoxic lipid A of *Rhodobacter capsulatus* 37b4. *Eur. J. Biochem.* 180:519–526.

Kröner, E. E., B. A. Peskar, H. Fischer, and E. Ferber. 1981. Control of arachidonic acid accumulation in bone marrow-derived macrophages by acyltransferases. *J. Biol. Chem.* 256:3690–3697.

Lewis, B. A., and D. M. Engelman. 1983. Lipid bilayer thickness varies linearly with acyl chain length in fluid phosphatidylcholine vesicles. *J. Mol. Biol.* 166:211–217.

Lien, E., T. K. Means, H. Heine, A. Yoshimura, S. Kusumoto, K. Fukase, M. J. Fenton, M. Oikawa, N. Qureshi, B. Monks, R. W. Finberg, R. R. Ingalls, and D. T. Golenbock. 2000. Toll-like receptor 4 imparts ligand-specific recognition of bacterial lipopolysaccharide. *J. Clin. Invest.* 105:497–504.

Loppnow, H., L. Brade, H. Brade, E. T. Rietschel, S. Kusumoto, T. Shiba, and H. D. Flad. 1986. Induction of human interleukin 1 by bacterial and synthetic lipid A. *Eur. J. Immunol.* 16:1263–1267.

Luzzati, V. 1997. Biological significance of lipid polymorphism: the cubic phases. *Curr. Opin. Struct. Biol.* 7:661–668.

Mantsch, H. H., and R. N. McElhaney. 1991. Phospholipid phase transitions in model and biological membranes as studied by infrared spectroscopy. *Chem. Phys. Lipids.* 57:213–226.

Mathison, J. C., P. S. Tobias, E. Wolfson, and R. J. Ulevitch. 1992. Plasma lipopolysaccharide (LPS)-binding protein: a key component in macrophage recognition of Gram-negative LPS. *J. Immunol.* 149:200–206.

Matsuura, M., M. Kiso, and A. Hasegawa. 1999. Activity of monosaccharide lipid A analogues in human monocytic cells as agonists or antagonists of bacterial lipopolysaccharide. *Infect. Immun.* 67:6286–6292.

McIntosh, T. J. 1980. Differences in hydrocarbon chain tilt between hydrated phosphatidylethanolamine and phosphatidylcholine bilayers. A molecular packing model. *Biophys. J.* 29:237–245.

Nakatsuka, M., Y. Kumazawa, M. Matsuura, J. Y. Homma, M. Kiso, and A. Hasegawa. 1989. Enhancement of nonspecific resistance to bacterial infections and tumor regressions by treatment with synthetic lipid A-subunit analogs. Critical role of *N*- and 3-*O*-linked acyl groups in 4-*O*-phosphono-D-glucosamine derivatives. *Int. J. Immunopharm.* 11: 349–358.

Poxon, S. W., and J. A. Hughes. 1999. Characterization of endotoxin and cationic liposome interaction. *Pharmacol. Devel. Tech.* 4:135–143.

Rietschel, E. T., H. Brade, O. Holst, L. Brade, S. Müller-Loennies, U. Mamat, U. Zähringer, F. Beckmann, U. Seydel, K. Brandenburg, A. J. Ulmer, T. Mattern, H. Heine, J. Schletter, S. Hauschildt, H. Loppnow, U. Schönbeck, H.-D. Flad, U. F. Schade, F. Di Padova, S. Kusumoto, and R. R. Schumann. 1996. Bacterial endotoxin: chemical constitution, biological recognition, host response, and immunological detoxification. *Curr. Top. Microbiol. Immunol.* 216:39–81.

Schindler, U., and V. R. Baichwal. 1994. Three NF-kappa B binding sites in the human E-selectin gene required for maximal tumor necrosis factor-α-induced expression. *Mol. Cell. Biol.* 14:5820–5831.

Schromm, A. B., K. Brandenburg, H. Loppnow, A. P. Moran, M. H. J. Koch, E. T. Rietschel, and U. Seydel. 2000. Biological activities of lipopolysaccharides are determined by the shape of their lipid A portion. *Eur. J. Biochem.* 267:2008–2013.

Schromm, A. B., K. Brandenburg, H. Loppnow, U. Zähringer, E. T. Rietschel, S. F. Carroll, M. H. J. Koch, S. Kusumoto, and U. Seydel. 1998. The charge of endotoxin molecules influences their conformation and interleukin-6 inducing capacity. *J. Immunol.* 161:5464–5471.

Schromm, A. B., K. Brandenburg, E. T. Rietschel, H.-D. Flad, S. F. Carroll, and U. Seydel. 1996. Lipopolysaccharide binding protein (LBP) mediates CD14-independent intercalation of lipopolysaccharide into phospholipid membranes. *FEBS Lett.* 399:267–271.

Schromm, A. B., E. Lien, P. Henneke, J. C. Chow, A. Yoshimura, H. Heine, E. Latz, B. G. Monks, D. A. Schwartz, K. Miyake, and D. T. Golenbock. 2001. Molecular genetic analysis of an endotoxin nonresponder mutant cell line: a point mutation in a conserved region of MD-2 abolishes endotoxin-induced signaling. *J. Exp. Med.* 194:79–88.

Seydel, U., M. Oikawa, K. Fukase, S. Kusumoto, and K. Brandenburg. 2000. Intrinsic conformation of lipid A is responsible for agonistic and antagonistic activity. *Eur. J. Biochem.* 267:3032–3039.

Seydel, U., O. Scheel, M. Müller, K. Brandenburg, and R. Blunck. 2001. A K^+ channel is involved in LPS signaling. *J. Endotox. Res.* 7:243–247.

Shimazu, R., S. Akashi, H. Ogata, Y. Nagai, K. Fukudome, K. Miyake, and M. Kimoto. 1999. MD-2, a molecule that confers lipopolysaccharide responsiveness on Toll-like receptor 4. *J. Exp. Med.* 189:1777–1782.

Takada, H., S. Kotani, S. Tanaka, T. Ogawa, I. Takahashi, M. Tsujimoto, T. Komuro, T. Shiba, S. Kusumoto, and N. Kusunose. 1988. Structural requirements of lipid A species in activation of clotting enzymes from the horseshoe crab, and the human complement cascade. *Eur. J. Biochem.* 175:573–580.

Tobias, P. S., and R. J. Ulevitch. 1993. Lipopolysaccharide binding protein and CD14 in LPS-dependent macrophage activation. *Immunobiology.* 187:227–232.

Triantafilou, K., M. Triantafilou, and R. L. Dedrick. 2001. A CD14-independent LPS receptor cluster. *Nat. Immunol.* 2:338–345.

Yang, R. B., M. R. Mark, A. Gray, A. Huang, M. H. Xie, M. Zhang, A. Goddard, W. I. Wood, A. L. Gurney, and P. J. Godowski. 1998. Toll-like receptor-2 mediates lipopolysaccharide-induced cellular signaling. *Nature.* 395:284–288.

Yoshimura, A., E. Lien, R. R. Ingalls, E. Tuomanen, R. Dziarski, and D. T. Golenbock. 1999. Cutting edge: recognition of Gram-positive bacterial cell wall components by the innate immune system occurs via Toll-like receptor 2. *J. Immunol.* 163:1–5.

Zähringer, U., B. Lindner, and E. T. Rietschel. 1994. Molecular structure of lipid A, the endotoxic center of bacterial lipopolysaccharides. *Adv. Carbohydr. Chem. Biochem.* 50:211–276. leads to a broader distribution of the backbone and the estimation of S provides an upper limit.